Calculating properties with the polymorphous coherent-potential approximation

B. Ujfalussy
Metals and Ceramics Division, Oak Ridge National Laboratory, Oak Ridge, Tennessee 37830

J. S. Faulkner
Alloy Research Center and Department of Physics, Florida Atlantic University, Boca Raton, Florida 33431

N. Y. Moghadam and G. M. Stocks
Metals and Ceramics Division, Oak Ridge National Laboratory, Oak Ridge, Tennessee 37830

Yang Wang
Pittsburgh Supercomputing Center, Pittsburgh, Pennsylvania 15213
(Received 21 May 1999; revised manuscript received 10 February 2000)

The formulas for calculating properties of an alloy such as the density of states, the charge density, and the Bloch spectral density function are derived from multiple-scattering theory for the polymorphous coherent-potential approximation (PCPA). The chemical shifts obtained for three alloy systems using the PCPA, the Korringa-Kohn-Rostoker CPA, and the locally self-consistent multiple-scattering method are compared with experiment. A significant improvement in the treatment of Coulomb effects is achieved using the PCPA with only a little more computational effort than for the older isomorphous CPA's.

I. INTRODUCTION

The one-electron method based on the density-functional theory and the local-density approximation[1] (DFT-LDA) is used routinely to calculate the energetics of ordered crystalline solids. These band-theory methods cannot be used to treat disordered solids, even such conceptually simple ones as substitutional solid-solution alloys, because of the lack of long-range order. Faced with this situation, many researchers turn to completely different approaches in their quest to explain the properties of alloy systems. Some introduce heuristic models with parameters that are obtained from fitting to observations.[2] Others carry out DFT-LDA calculations on intermetallic compounds having relatively small numbers of atoms in the unit cells with the purpose of interpolating the energetics of the infinite disordered system from those of the ordered solids.[3] Today, the electronic structure for models of disordered solids can be calculated using supercells that contain thousands of atoms. This has been made possible by the development of order-N methods based on plane-wave expansions[4] or multiple-scattering theory.[5] Still, it is useful for certain applications, and more satisfying philosophically, to have a simple approximate theory that will describe the important features of the electronic structure of alloys. Exact calculations on one-dimensional and three-dimensional models of alloys, as well as more mathematical considerations,[6] convinced theorists that the coherent-potential approximation[7] (CPA) provides such a simple approximate theory.

The CPA calculations on solvable models of alloys give qualitative guidance for the interpretation of experiments on real alloys, but to make the predictions quantitative it was necessary to merge the CPA with the Korringa-Kohn-Rostoker[8] (KKR) band theory method.[9] The KKR-CPA was later extended to produce self-consistent one-electron potentials.[10] Care was taken to insure that they satisfy the requirement of the DFT-LDA that they are obtained as functional derivatives of the potential energy with respect to the local charge densities. The addition of a self-consistency step, however, brings in an aspect of the CPA theory that had never been considered before.

In order to understand the difficulties involved with including charge self-consistency in a CPA, it is necessary to be aware that all of the model calculations and mathematical studies of the CPA made use of isomorphous models of alloys. An isomorphous model is one in which, for a binary alloy, the A atoms are all assumed to have identical charge densities $\rho_A(\mathbf{r})$ and hence potential functions $\nu_A(\mathbf{r})$, and the B atoms all have identical $\rho_B(\mathbf{r})$ and $\nu_B(\mathbf{r})$. In the CPA, a scattering matrix $\hat{\mathbf{t}}_A(\mathbf{t}_c)$ is calculated for an A atom embedded in a lattice with the effective t matrix $\mathbf{t}_c$ on all the other sites. The scattering matrix for an A atom embedded in a vacuum, which appears in $\hat{\mathbf{t}}_A(\mathbf{t}_c)$, is calculated in the usual way from the potential $\nu_A(\mathbf{r})$. The scattering matrix $\hat{\mathbf{t}}_B(\mathbf{t}_c)$ is calculated analogously. The desired t matrix, $\mathbf{t}_c$, is obtained from the null scattering requirement, $c_A\hat{\mathbf{t}}_A(\mathbf{t}_c)+c_B\hat{\mathbf{t}}_B(\mathbf{t}_c)=0$. The assumption of isomorphous models was so ubiquitous that theorists made it without thinking.

It is known from band-theory calculations on ordered intermetallic compounds that there is a charge transfer between the different species of atoms, and this leads to a Madelung contribution to the self-consistent potentials. The net charges on the A and B sites are $q_A=\int\rho_A(\mathbf{r})d\mathbf{r}-Z_A$ and $q_B=\int\rho_B(\mathbf{r})d\mathbf{r}-Z_B$, where the integrals are over the unit cells and the Z's are the atomic numbers. The charge self-consistent KKR-CPA method also predicts nonzero net charges, but it contains a curious inconsistency in that there is no Madelung potential in it. A careful analysis shows that the derivation of self-consistent potentials in a disordered

alloy subject to the condition that the resulting model must be isomorphic leads inevitably to the conclusion that the Madelung potentials must be zero. In addition to the arguments in the original derivations,[10] a way of understanding this paradoxical result is to note that any distribution of charged atoms will give a different Madelung potential at each site, irrespective of the kind of atom at the site. The only way for all the *A* atoms to have the same potential and all the *B* atoms to have another, as required by the isomorphous model, is to approximate the Madelung contributions with zero. It was understood at the time that the isomorphous picture was only an approximation. However, the technology to test such ideas had not yet been developed, and it was hoped that the fluctuations about the average charges would be small.

The isomorphous KKR-CPA was criticized because the Madelung potentials were set equal to zero,[11] and efforts were made to deal with this criticism. These led to two very similar methods, the screened-impurity model[12] CPA (SIM-CPA) and the screened CPA (S-CPA).[13] Both of these models are isomorphous, and the Madelung potential is calculated by placing a shell of charge around each atom at a radius $R_{\rm eff}$. The total charge on the shell is equal to the charge on the atom. Using calculations on the screening of single impurities in an otherwise perfect crystal as a guide,[14] the effective radius is usually chosen to be equal to radius of the nearest-neighbor shell R_1. The resulting self-consistent potentials contain a Madelung term, and there is a Coulomb contribution to the total energy. The charge transfers q_A and q_B predicted by the SIM-CPA and S-CPA are different from the ones obtained from the KKR-CPA, and they improve the agreement with many experiments. If one accepts the argument that the mathematically correct value for the Madelung potential in an isomorphous model of an alloy is zero, as derived in Ref. 10, the derivations of the isomorphous SIM-CPA and S-CPA must contain inconsistencies. There is a sense in which the SIM-CPA and S-CPA can be justified, and that will be explained below.

The environment for developing theories of alloys changed dramatically with the advent of the order-*N* calculations mentioned above.[4,5] Using a technique called the locally self-consistent multiple-scattering method (LSMS),[15] first-principles DFT-LDA calculations on models of alloys using supercells that contain hundreds or even thousands of atoms have been carried out.[16–18] Figure 1 of Ref. 18 shows the distribution of atomic charges q^i for a 50% copper-zinc alloy on a fcc Bravais lattice calculated with a supercell containing 500 atoms. It is seen that there is quite a broad distribution of charges on the sites, and the numerical output shows that the q^i are different for every site *i*. Of course, *q* falls within one range of values if there is an *A* atom on site *i*, and another range if there is a *B* atom there. It follows that an alloy is more properly described by a polymorphous model in which the charge density $\rho^i(\mathbf{r})$ on every site is unique. This result was anticipated to some extent in Ref. 11, although those authors deduced from their calculations on supercells containing 4–12 atoms that the number of possible charges that a given kind of atom can have is small and depends only on the occupation of the sites in the nearest-neighbor shell. It is shown in Fig. 2 of Ref. 17 that the Madelung potential at any lattice site is not screened at the nearest-neighbor shell radius. Instead, the contributions to this potential from succeeding shells diminish very slowly. It is demonstrated in that same reference that a part of the Coulomb energy has a contribution u_{C1} that depends only on the average charge transfer, as would be anticipated from an isomorphous CPA, but it is also demonstrated that there is a contribution u_{C2} that is not determined by the average charge transfer but depends on the distribution of the charges about the average.

Isomorphous CPA models have been remarkably successful in explaining many interesting properties of alloys,[6] and some of the reasons for that are given in Ref. 18. Even though the Madelung potentials are set equal to zero in the KKR-CPA, that approximation gives surprisingly good values for the free energy of mixing. Another curve in Fig. 2 of Ref. 17 shows that the average of the Madelung potentials for all the *A* sites or *B* sites in the alloy is short range as assumed in the SIM-CPA and S-CPA. The parameter $R_{\rm eff}$ turns out to be approximately equal to R_1, and this explains the successes that these isomorphous CPA's have had. On the other hand, locating the screening charge on a shell is clearly an approximation, and defining $R_{\rm eff}$ to be R_1 makes the SIM-CPA and S-CPA theories precise but removes the possibility for improving them by treating $R_{\rm eff}$ as an adjustable parameter. In addition, it has been shown that the form for the total Coulomb energy that arises naturally in the models is unsatisfactory. In the SIM-CPA, the expression is multiplied by an adjustable parameter β that cannot be obtained from within the theory.[19] It is even more disturbing that this parameter multiplies the Coulomb energy, but it does not occur in the one-electron potential. This violates the requirement of the DFT-LDA that the one-electron potential is the functional derivative of the energy with respect to the charge density. The parameter β can be understood as an effort to emulate the contribution u_{C2} to the Coulomb energy within the limitations of an isomorphous CPA.[20]

Because of the theoretical objections to isomorphous models, it was suggested in Ref. 18 that Coulomb effects could be included better at the level of the coherent-potential approximation with a polymorphous CPA (PCPA) than with any isomorphous CPA. The PCPA will generate charge densities $\rho_{A,i}(\mathbf{r})$ and $\rho_{B,i}(\mathbf{r})$ and hence potential functions $\nu_{Ai}(\mathbf{r})$ and $\nu_{Bi}(\mathbf{r})$ that are different for every site in the alloy, as found from the first-principles LSMS calculations. The theory of the PCPA was deduced from a careful study of the results of order-*N* calculations, so it is necessary to describe some of the inner workings of the order-*N* methods in more detail.

The LSMS makes use of the principle of near-sightedness that has been espoused by Kohn[21] insofar as the continuity of the wave functions is concerned. Infinitely many atoms are included in the calculation, with supercells containing *N* atoms being reproduced periodically to fill all space. The multiple-scattering equations are solved completely for all the atoms in a local interaction zone (LIZ) surrounding a given atom. The *t* matrices for the sites outside the LIZ are set equal to zero. This process is repeated for LIZ's centered on each atom in the supercell, which makes the calculation order-*N*. The principle of near-sightedness is not used in the Coulomb part of the calculation. The Madelung potential for each site is calculated exactly with the contributions from the

full infinity of atomic charges, not just the ones in the LIZ, being included. It could be said that the multiple-scattering part of the calculation is order-N, but the Coulomb part is not. The Madelung potentials for solids with periodic boundary conditions are easy to calculate with the Ewald method,[22] so that does not slow down the overall procedure.

A locally self-consistent Greens function (LSGF) method has been suggested,[23] which was influenced by the success of the LSMS. In the LSGF, the LIZ's are made smaller by putting an effective scatterer on the sites outside the LIZ, rather than zero as in the LSMS. A reasonable choice, although not the only choice, for this scattering matrix is a CPA t matrix $\mathbf{t}_c$.[24] As is the case in the LSMS the Madelung potentials are calculated exactly, the sums including the infinity of atomic charges. Placing the effective scatterers on the sites of a Bravais lattice outside the LIZ limits the LSGF to systems for which the atomic sites are periodic, while the LSMS can be applied to systems in which the atoms have arbitrary atomic positions, such as bulk amorphous solids.[25] The LSMS must also be used for systems for which a homogeneous alloy is a poor reference medium, such as magnetic multilayers and interfaces,[26] and magnetic noncollinearity.[27] The LSGF is clearly the best method for the study of disordered substitutional alloys, and it predicts the same electronic structure as the LSMS if both methods are converged. In particular, the model of an alloy produced by a LSGF calculation is also polymorphous, and this holds for LSGF calculations in which the LIZ is chosen to contain only one atom. As pointed out in Ref. 18, it is the authors position that the particular kind of LSGF calculation in which the effective scatterer is determined by the CPA condition and the LIZ contains one atom has the shape that is needed for a PCPA. The originators of the LSGF did not have the construction of a PCPA as one of their goals because, among other things, they are also the originators of the SIM-CPA.[23,24,12]

It is reasonable for an expert in the CPA to worry that, while the PCPA should lead to an improved treatment of Coulomb effects and give a physically more correct picture of the alloy, all of the other desirable features of the CPA that have been so useful in applications over many years will be lost. The main purpose of this paper is to develop a mathematical formalism which leads to the PCPA and from which the site-diagonal and non-site-diagonal average Green's functions are obtained. These Green's functions are different from the ones derived for the isomorphous CPA because charge correlations are built into them, but they can be used equally well to calculate the properties of alloys. A rather subtle point that comes from the formalism is that full potentials (i.e., not muffin-tin) can be used in PCPA calculations, while they cannot in isomorphous CPA calculations.

The formulas for calculating properties of an alloy such as the density of states, the charge density, and the Bloch spectral density function with an isomorphous CPA were derived from multiple-scattering theory in a paper that will be referred to as FS.[28] In the following section, the analogous formulas will be derived for the PCPA. The differences between the two sets of formulas for the non-site-diagonal Green's function and the Bloch spectral density function $A^B(E,\mathbf{k})$ are particularly interesting. It is demonstrated that the manipulation of the DFT-LDA Green's function for an alloy under the class of restrictions that define a CPA leads to the PCPA. If the additional restriction that the resulting model must be isomorphous is invoked, the result is the KKR-CPA. The S-CPA and SIM-CPA do not fit into this chain of approximations, although, as mentioned above, they are useful approximations.

Calculations of various alloy parameters have been carried out with the LSGF within the tight-binding linear muffin-tin orbital (TB-LMTO) method, and the LIZ was chosen to contain one atom in some of these. Calculations based on the multiple-scattering theory, which is the natural language of the CPA method, will be shown in this paper. The use of this method makes it easier to compare with LSMS and KKR-CPA results. In Sec. III, some of the details of the computational methods are described. In a previous paper,[29] it was shown that the chemical shifts in alloys are a particularly sensitive measure of the Coulomb effects. The chemical shifts obtained from the KKR-CPA, PCPA, and LSMS are compared with experiment in Sec. IV. The atomic charges predicted by the three theories in real alloy systems are also compared with each other. In the last section, the argument is made that the PCPA gives useful results with only a little more effort than the older isomorphous CPA's, and other aspects of the theory are discussed.

II. CALCULATING PROPERTIES WITH THE PCPA

A. The Green's function for alloys

The DFT-LDA Schrödinger equation for a collection of N atoms can be written as

$$\left[-\nabla^2+\sum_{i=1}^{N}\nu_i(\mathbf{r})\right]\psi(\mathbf{r})=E\psi(\mathbf{r}), \tag{1}$$

where the one-electron potentials will be assumed to have the muffin-tin form. Multiple-scattering theory can deal with more general potentials, such as atomic-sphere approximation (ASA) potentials or even full potentials, but the notation becomes complex. The atomic potential $\nu_n(\mathbf{r}_n)$, where $\mathbf{r}_n=\mathbf{r}-\mathbf{R}_n$, is spherically symmetric when $\mathbf{r}$ is within a sphere centered on the lattice site $\mathbf{R}_n$, and is zero otherwise. One way to write the corresponding Green's function was shown in FS to be

$$G(E,\mathbf{r},\mathbf{r}')=\sum_{L,L'}Z_L^n(E,\mathbf{r}_n)\tau_{LL'}^{nn}Z_{L'}^n(E,\mathbf{r}_n')-\sum_{L}Z_L^n(E,\mathbf{r}_n)J_L^n(E,\mathbf{r}_n'). \tag{2}$$

In this equation, $Z_L^n(E,\mathbf{r})$ is the solution of

$$[-\nabla^2+\nu_n(\mathbf{r})-E]Z_L^n(\mathbf{r})=0, \tag{3}$$

that is regular at the origin and equals

$$Z_L^n(E,\mathbf{r})=Y_L(\mathbf{r})j_l(\kappa r)m_l^n(E)-i\kappa Y_L(\mathbf{r})h_l(\kappa r), \tag{4}$$

when r is greater than the radius of the nth muffin-tin sphere. It is assumed in Eq. (2) that $r_n'>r_{\mathbf{n}}$. The matrix $\mathbf{m}^n(E)$ is the inverse of the t matrix $\mathbf{t}^n$ that describes the scattering from the potential $\nu_n(\mathbf{r})$. Since $\mathbf{t}^n$ is diagonal for muffin-tin poten-

tials, its inverse is as well, and m_l^n is a diagonal element of that matrix. The functions $j_l(\kappa r)$ and $h_l(\kappa r)$ are Bessel functions, and κ is the square root of the energy. Following FS, the spherical harmonics $Y_L(\mathbf{r})$ are chosen to be real. The function $J_L^n(E,\mathbf{r})$ is the solution of Eq. (1) that is not regular at the origin and approaches $Y_L(\mathbf{r})j_l(\kappa r)$ when r is greater than the radius of the nth muffin-tin sphere. The coefficients $\tau_{LL'}^{nm}$ are elements of the scattering-path matrix defined below. This form of the Green's function is valid when $\mathbf{r}$ and $\mathbf{r}'$ are inside the nth muffin-tin sphere or in the interstitial region between the muffin-tin spheres, where the potential is zero.

The same Green's function can be written in a different way when $\mathbf{r}$ is in the nth muffin-tin sphere and $\mathbf{r}'$ is in the mth sphere, or they are in the interstitial region. For this case, the Green's function is

$$G(E,\mathbf{r},\mathbf{r}')=\sum_{L,L'} Z_L^n(E,\mathbf{r}_n)\tau_{LL'}^{nm}Z_{L'}^m(E,\mathbf{r}'_m). \tag{5}$$

The expressions for the Green's functions in Eqs. (2) and (5) have been used in a wide range of calculations, and are reliable. Clearly, the convergence of the sums becomes a problem if the magnitudes of the position vectors are too large.

The elements of the scattering-path matrix, $\tau_{LL'}^{nm}(E)$, are most easily obtained by taking the inverse of the matrix

$$M_{LL'}^{nm}=m_l^n\delta_{LL'}\delta_{nm}-g_{LL'}^{nm}. \tag{6}$$

That is to say,

$$\tau_{LL'}^{nm}=[\mathbf{M}^{-1}]_{LL'}^{nm}. \tag{7}$$

The functions $g_{LL'}^{nm}$ are components of the free-electron Green's functions that describe propagation from lattice sites $\mathbf{R}_n$ to $\mathbf{R}_m$, and are zero when $n=m$. The elements of the inverse of the t matrix on site $\mathbf{R}_n$, m_l^n, were defined above.

B. The averaging process

A theory of the electronic states in a disordered alloy must have a statistical as well as a quantum-mechanical aspect because the knowledge about the structure of such a system will, of necessity, be incomplete. In the ideal random alloy, which is considered here, the atoms are distributed on the sites of a Bravais lattice. The probability of an A or B atom occupying a site is c_A or c_B. In more realistic models, the Warren-Cowley short-range order coefficients measure the deviation from a random distribution.

A major difference between the isomorphous CPA and the PCPA is the nature of the averaging process used in the statistical stage. It was natural in FS to use an ensemble-averaging process, the ensemble being the set of $(N_A+N_B)!/N_A!N_B!$ alloys that can be formed by distributing $N_A A$ atoms and $N_B B$ atoms on the lattice sites, and then passing to the limit that N_A and N_B approach infinity. In the PCPA, the average is over the sites of one infinitely large sample. The reason for this type of averaging is that the only reliable way to calculate the Madelung potential at a site is to include the contributions from the charges on all the other sites. This is the lesson that has been learned from the LSMS, the LSGF, and other order-N techniques, as was described in the previous section. This point will be made even more clearly in Sec. II D, where the calculation of the self-consistent potential in the PCPA is discussed in more detail. The difference between the various A and B atoms is due to their spatial correlation with all of the other atoms, and information about this spatial correlation is lost in the kind of ensemble-averaging process used in FS. The site-averaged Green's function will be seen to be periodic, as it should be.

Since the properties of interest are self-averaging, the ensemble- and site-averaging processes lead to the same results when applied to the same model. The concept of self-averaging is used frequently in modern discussions of statistical physics, but it first appeared in alloy theory in the writings of Lifshitz.[30] The argument was made in FS that the ensemble-averaged quantities should represent the properties of a single real crystal because of self-averaging. For the PCPA, it is necessary to argue that average values for properties can be found from one large sample because of self-averaging.[31] It will be shown in the following that formulas derived with the site-averaging process become identical to those derived with ensemble averaging when the model is taken to be isomorphous.

C. Averaging the Green's function for the site-diagonal case

Using the site-averaging process, the average of the Green's function defined in Eq. (2) over all the N sites in a volume V of the large sample is

$$\langle G(E,\mathbf{r},\mathbf{r}')\rangle=\frac{1}{N}\sum_{\substack{i=1\\ i\subset V}}^{N}\left[\sum_{L,L'} Z_L^i(E,\mathbf{r})\tau_{LL'}^{ii}Z_{L'}^i(E,\mathbf{r}')-\sum_L Z_L^i(E,\mathbf{r})J_L^i(E,\mathbf{r}')\right]. \tag{8}$$

In each term in the sum over i, the origin of the coordinate system is moved to the lattice position $\mathbf{R}_i$. The limit of this process is reached as N and hence V increase without bound. It should be clear that this averaged Green's function is periodic, $\langle G(E,\mathbf{r},\mathbf{r}')\rangle=\langle G(E,\mathbf{r}+\mathbf{R}_n,\mathbf{r}'+\mathbf{R}_n)\rangle$, because the sum is unchanged.

Approximating this averaged Green's function using the philosophy of the coherent-potential approximation entails simplifying the scattering-path matrix elements in a specific way. As was discussed in FS, the single-site approximation to the scattering-path matrix leads to a redefinition of the matrix elements $\tau_{LL'}^{ii}$ so that they are given by the inverse of a matrix $\mathbf{M}_c^i$ whose elements are given by

$$\mathbf{M}_c^{i,ii}=\mathbf{m}^i \quad \text{for } n=i,\ m=i,$$

$$\mathbf{M}_c^{i,nm}=\mathbf{m}^c\delta_{nm}-\mathbf{g}^{nm} \quad \text{for } n\neq i, \text{ or } m\neq i, \tag{9}$$

in a block-matrix notation that eliminates the angular momentum indices. The matrix $\mathbf{m}^i$ is the inverse of the t matrix that defines scattering from the potential $\nu_i(\mathbf{r})$, and the matrix $\mathbf{m}^c$ is the inverse of the effective scatterer $\mathbf{t}_c$. Another way to write this scattering-path operator is

$$\tau^{ii}\rightarrow\tau_c^{i,00}=\mathbf{D}^i\tau_c^{00}=\tau_c^{00}\tilde{\mathbf{D}}^i, \tag{10}$$

where

$$\mathbf{D}^i=[I+\tau_c^{00}(\mathbf{m}^n-\mathbf{m}^c)]^{-1}. \tag{11}$$

As discussed in Sec. I, the CPA averaged Green's function describes a periodic system with the scattering matrix $\mathbf{t}_c$ on every site. The matrix τ_c^{nm} is the scattering-path matrix for this system, and is obtained from the inverse of the matrix $\mathbf{M}_c$ with elements

$$\mathbf{M}_c^{nm}=\mathbf{m}^c\boldsymbol{\delta}_{nm}-\mathbf{g}^{nm} \text{ for all } n \text{ and } m. \tag{12}$$

Since this system is periodic, $\tau_c^{ii}=\tau_c^{jj}=\tau_c^{00}$.

The site-diagonal average Green's function in the single-site approximation is then

$$G^{\mathrm{SD}}(E,\mathbf{r},\mathbf{r}')=\frac{1}{N}\sum_{\substack{i=1\\ i\subset V}}^{N}\left[\sum_{L,L'} Z_L^i(E,\mathbf{r})\tau_{c,LL'}^{i,00}Z_{L'}^i(E,\mathbf{r}')-\sum_L Z_L^i(E,\mathbf{r})J_L^i(E,\mathbf{r}')\right]. \tag{13}$$

The average density of states per site for the alloy is an example of a site-diagonal property, and it can be found from this Green's function by

$$\langle n(E)\rangle=-\frac{1}{\pi}\mathrm{Im}\int_\Omega G^{\mathrm{SD}}(E,\mathbf{r},\mathbf{r})dv, \tag{14}$$

where Ω is the volume of the central unit cell. Clearly, the density of states associated with any site in the effective crystal is the average of that quantity for the individual atoms in V

$$\langle n(E)\rangle=\frac{1}{N}\sum_{i=1}^{N} n^i(E), \tag{15}$$

where

$$n^i(E)=-\frac{1}{\pi}\mathrm{Im}\left[\sum_{L,L'}\int_\Omega Z_L^i(E,\mathbf{r})Z_{L'}^i(E,\mathbf{r})d\mathbf{r}\tau_{LL'}^{i,00}\right]. \tag{16}$$

The charge density on a site in the effective crystal is similarly

$$\langle\rho(\mathbf{r})\rangle=\frac{1}{N}\sum_{i=1}^{N}\rho^i(\mathbf{r}), \tag{17}$$

where

$$\rho^i(\mathbf{r})=-\frac{1}{\pi}\int_{-\infty}^{E_F}\mathrm{Im}\left[\sum_{L,L'} Z_L^i(E,\mathbf{r})Z_{L'}^l(E,\mathbf{r})\tau_{LL'}^{i,00}(E)\right]dE. \tag{18}$$

The term in Eq. (13) that includes the singular solution $J_L^i(E,\mathbf{r})$ normally does not appear in formulas for properties because it is real.

As stated above, Eq. (13) should become identical with the corresponding KKR-CPA equation when it is applied to an isomorphous model. For that case, the functions of position $Z_L^i(E,\mathbf{r})$ and $J_L^i(E,\mathbf{r})$ are all $Z_L^A(E,\mathbf{r})$ and $J_L^A(E,\mathbf{r})$ when there is an A atom on the ith site or $Z_L^B(E,\mathbf{r})$ and $J_L^B(E,\mathbf{r})$ when a B atom is there. This is equivalent to the assumption that the potentials on all the A or B sites are $\nu_A(\mathbf{r})$ or $\nu_B(\mathbf{r})$, and hence the t matrices are $\mathbf{t}^A$ or $\mathbf{t}^B$. The resulting equation is

$$G_{\mathrm{iso}}^{\mathrm{SD}}(E,\mathbf{r},\mathbf{r}')=\sum_{L,L'}\left[c_A Z_L^A(E,\mathbf{r})\tau_{LL'}^{A,00}Z_{L'}^A(E,\mathbf{r}')+c_B Z_L^B(E,\mathbf{r})\tau_{LL'}^{B,00}Z_{L'}^B(E,\mathbf{r}')\right]-\sum_L\left[c_A Z_L^A(E,\mathbf{r})J_L^A(E,\mathbf{r}')+c_B Z_L^B(E,\mathbf{r})J_L^B(E,\mathbf{r}')\right], \tag{19}$$

which is identical with Eq. (2.33) of FS. The most obvious difference between the Eqs. (13) and (19) is that in the PCPA all the atoms are assumed to be unique, and hence their concentrations are just $1/N$. The formulas that are the analog of Eqs. (15) and (17) are

$$\langle n(E)\rangle=c_A n^A(E)+c_B n^B(E) \tag{20}$$

and

$$\langle\rho(\mathbf{r})\rangle=c_A\rho^A(\mathbf{r})+c_B\rho^B(\mathbf{r}). \tag{21}$$

The Green's functions defined in Eqs. (13) and (19) are periodic, as they should be, $G_{\mathrm{iso}}^{\mathrm{SD}}(E,\mathbf{r},\mathbf{r}')=G_{\mathrm{iso}}^{\mathrm{SD}}(E,\mathbf{r}+\mathbf{R}_n,\mathbf{r}'+\mathbf{R}_n)$.

D. The PCPA condition and self-consistency

To this point, the single-site approximation has been used, but nothing has been said about the definition of the effective scattering matrix $\mathbf{t}_c$. The relation that defines $\mathbf{t}_c$ in the isomorphous CPA appears in Eq. (5.24) of FS as

$$c_A\tau_c^{A,00}+c_B\tau_c^{B,00}=\tau_c^{00}, \tag{22}$$

where $\tau^{A,00}$ is obtained from Eqs. (9) by putting the inverse of the scattering matrix for the potential $\nu_A(\mathbf{r})$ on the central site and $\tau^{B,00}$ is obtained similarly. This is just the conversion of the original definition of the CPA (Ref. 7) into the language of the multiple-scattering theory.[32] The extension of this relation that defines the effective scattering matrix in the PCPA is

$$\frac{1}{N}\sum_{i=1}^{N}\tau_c^{i,00}=\tau_c^{00}, \tag{23}$$

where the scattering-path matrices are defined in Eq. (10).

The information necessary for calculating self-consistent potentials and total energies in the PCPA is contained in the site-diagonal Green's functions in Eq. (13). As in any other system in which there is charge transfer, the local part of the DFT-LDA potential $\nu_i(\mathbf{r})$ is calculated from the charge density $\rho^i(\mathbf{r})$ defined in Eq. (18). The Madelung contribution is defined using the net charges $q^j=\int\rho^j(\mathbf{r})d\mathbf{r}-Z_j$ for all $j\neq i$, where $Z_j=Z_A$ if there is an A atom on the jth site, and $Z_j=Z_B$ if there is a B atom on the site. This is the same way that $\nu_i(\mathbf{r})$ is calculated in the LSMS or the LSGF.

In practical applications of the PCPA, the charge densities $\rho^i(\mathbf{r})$ and potentials $\nu_i(\mathbf{r})$ cannot be calculated for N equal to infinity, so it is necessary to make a supercell approximation.

In this approximation, the configuration of atoms in the central supercell is reproduced periodically to fill all space. This same approximation is made in order-N methods, such as the LSMS and LSGF. The use of supercells does not interfere with the periodicity of the Green's functions demonstrated in the previous paragraph. The calculation of the Madelung potential for all the sites in the supercell takes very little time when the Ewald (Ref. 22) method is used. As a practical matter, calculations of interesting properties using supercells of various sizes have shown that the supercell approximation is not serious as long as the cells contain some hundreds of atoms. One reason for this is that the Madelung sums are not seriously affected if the actual contents of the adjoining supercells in the large sample are replaced with replicas of the central cell. Another is that the properties of interest in the calculations are self-averaging.

It may seem contradictory to talk about an effective crystal that is periodic, and at the same time talk about net charges on the sites. A similar contradiction occurs in the isomorphous CPA, because one uses $\rho_A(\mathbf{r})$ and $\rho_B(\mathbf{r})$ to calculate the DFT-LDA potential in spite of the fact that the effective scatterers on all the sites are the same. Ensuring this does not lead to a contradiction is the purpose of the CPA condition. The major point of FS is that this is a necessary part of the formalism. A quantity like the total density of states does not require knowledge of the wave functions and can be calculated from the periodic effective crystal with $\mathbf{t}_c$ on every site using Lloyd's formula.[33] Information about individual sites must be used in the calculation of a property that requires wave functions, such as the potentials, because there is no average wave function in an alloy, only an average Green's function.

E. Averaging the Green's function for the non-site-diagonal case

The most interesting non-site-diagonal properties are related to the Bloch spectral density function. The PCPA, like the isomorphous CPA, leads to an effective Green's function that is periodic. This means that Bloch vectors $\mathbf{k}$ should play a role in the theory, even though they are not good quantum numbers. The E vs $\mathbf{k}$ relation of ordinary band theory is replaced in alloy theory with the Bloch spectral density, which is the density of states in $\mathbf{k}$ space. The formulas for the Bloch spectral density function derived in FS and displayed in Eqs. (4.8) and (4.9) of that paper are

$$A^B(E,\mathbf{k}) = -(1/\pi)\,\mathrm{Im}\,G(E,\mathbf{k},\mathbf{k}), \tag{24}$$

where

$$G(E,\mathbf{k},\mathbf{k}) = \sum_n e^{i\mathbf{k}\cdot\mathbf{R}_n}\int_\Omega G(E,\mathbf{r},\mathbf{r}+\mathbf{R}_n)\,d\mathbf{r}. \tag{25}$$

In Eq. (25), the sum is over all Bravais lattice vectors $\mathbf{R}_n$, and the integral is over the central unit cell. It should be noted that $G(E,\mathbf{k},\mathbf{k})$ is not the Fourier transform of the Green's function, as is used, e.g., in the analysis of positron annihilation experiments.

The Green's function that must be used in $A^B(E,\mathbf{k})$ is obtained from Eq. (5) by means of the site-averaging process

$$\langle G(E,\mathbf{r},\mathbf{r}+\mathbf{R}_n)\rangle = \frac{1}{N}\sum_{i=1}^{N}\sum_{L,L'} Z_L^i(\mathbf{r})\,\tau_{LL'}^{ij}\,Z_{L'}^j(\mathbf{r}). \tag{26}$$

The sum is only over site i, because the site j is related to site i by $\mathbf{R}_j = \mathbf{R}_i + \mathbf{R}_n$. It is shown in Eq. (2.43) in FS that the single-site approximation to the scattering-path matrix in this equation is

$$\tau^{ij} = \mathbf{D}^i \tau_c^{ij} \tilde{\mathbf{D}}^j, \tag{27}$$

where τ_c^{ij} is the scattering path matrix for a periodic lattice that has the PCPA scattering matrix $\mathbf{t}_c$ on every site. This matrix is found from the inverse of the matrix $\mathbf{M}_c$ defined in Eq. (12), and depends only on the separation between sites i and j

$$\tau_c^{ij} = \tau_c(\mathbf{R}_{ij}) = [M_c^{-1}]^{ij}. \tag{28}$$

The matrix $\mathbf{D}^i$ is given in Eq. (11). Thus, the non-site-diagonal averaged Green's function is

$$G^{\mathrm{NSD}}(E,\mathbf{r},\mathbf{r}+\mathbf{R}_n) = \frac{1}{N}\sum_{i=1}^{N}\sum_{L_1,L_2}\sum_{L,L'} Z_{L_1}^i(\mathbf{r}) D_{L_1L}^i \tau_{c,LL'}^{ij} \tilde{D}_{L'L_2}^j Z_{L_2}^j(\mathbf{r}). \tag{29}$$

Inserting this in Eq. (25) leads to the expression for the averaged Green's function in the $\mathbf{k}$ representation

$$G(E,\mathbf{k},\mathbf{k}) = \int_\Omega G^{\mathrm{SD}}(E,\mathbf{r},\mathbf{r})\,d\mathbf{r} + \sum_{\substack{n\\ R_n\neq 0}} e^{i\mathbf{k}\cdot\mathbf{R}_n}\sum_{LL'} F_{LL'}(\mathbf{R}_n)\,\tau_{c,LL'}(\mathbf{R}_n), \tag{30}$$

where $G^{\mathrm{SD}}(E,\mathbf{r},\mathbf{r}')$ is defined in Eq. (13). In Eq. (30),

$$F_{LL'}(\mathbf{R}_n) = \frac{1}{N}\sum_{i=1}^{N}\sum_{L_1,L_2}\int_\Omega Z_{L_1}^i(\mathbf{r}) Z_{L_2}^j(\mathbf{r})\,d\mathbf{r} D_{L_1L}^i D_{L_2L'}^j, \tag{31}$$

which depends on $\mathbf{R}_n$ because $\mathbf{R}_j = \mathbf{R}_i + \mathbf{R}_n$. The matrix $\mathbf{F}(\mathbf{R}_n)$ has weight one in the sense that it is the sum of N integrals, but divided by N.

Specializing to the isomophous case, for which $Z_L^i(\mathbf{r}) = Z_L^A(\mathbf{r})$ with probability c_A and $Z_L^i(\mathbf{r}) = Z_L^B(\mathbf{r})$ with probability c_B, $F_{LL'}(\mathbf{R}_n)$ becomes

$$\begin{aligned} F_{LL'}^{cc} = {} & c_A^2 \sum_{L_1,L_2}\int_\Omega Z_{L_1}^A(\mathbf{r}) Z_{L_2}^A(\mathbf{r})\,d\mathbf{r} D_{L_1L}^A D_{L_2L'}^A \\ & + c_A c_B \sum_{L_1,L_2}\int_\Omega Z_{L_1}^A(\mathbf{r}) Z_{L_2}^B(\mathbf{r})\,d\mathbf{r} D_{L_1L}^A D_{L_2L'}^B \\ & + c_B c_A \sum_{L_1,L_2}\int_\Omega Z_{L_1}^B(\mathbf{r}) Z_{L_2}^A(\mathbf{r})\,d\mathbf{r} D_{L_1L}^B D_{L_2L'}^A \\ & + c_B^2 \sum_{L_1,L_2}\int_\Omega Z_{L_1}^A(\mathbf{r}) Z_{L_2}^B(\mathbf{r})\,d\mathbf{r} D_{L_1L}^A D_{L_2L'}^B, \end{aligned} \tag{32}$$

which does not depend on $\mathbf{R}_n$. The resulting formula for $G(E,\mathbf{k},\mathbf{k})$ is identical to Eq. (4.10) of FS, which means that the Bloch spectral densities will be the same.

It is reassuring that the formulas for $F^{cc}_{LL'}$ and $A^B(E,\mathbf{k})$ obtained with the site-averaging process are identical with the ones obtained with the ensemble-averaging process when the former are applied to an isomorphous model. When ensemble averaging is used, the sum in Eq. (26) is over sites i and j independently. Since the function $F^{cc}_{LL'}$ in Eq. (32) does not depend on $\mathbf{R}_n$, it can be factored out of the integral in Eq. (30). This makes the expression for the Bloch spectral density for the isomorphous case, Eq. (4.15) of FS, considerably easier to deal with computationally.

F. Beyond the PCPA

There are three steps in the derivations given above; the site-averaging process, the single-site approximation, and defining the effective scattering matrix $\mathbf{t}_c$ as the one given by Eq. (23). It should be observed that these steps are independent, and that different levels of theory can be obtained by truncating the derivation after step one or making different choices in step 3. In particular, after a LSMS calculation on a supercell has been carried out, the results can be inserted into Eqs. (8) and (26) to get site-diagonal and non-site-diagonal averaged Green's functions. These can be used directly to obtain such quantities as the Bloch spectral densities without making a single-site or a CPA approximation. The process of averaging reduces the amount of information in the LSMS results, but there are situations in which this is desirable. Experience with order-N calculations like the LSMS has demonstrated that there is frequently too much information in the results. The averaging process may be helpful in resolving the more important physical effects from the mass of computed data. The averaged Green's functions could also provide a good standard by which approximations like the PCPA can be tested.

It should also be noted that the site-averaging process may be applied to supercells that have short-range order or displacements of the atoms from their average lattice sites. It will have to be seen if these capabilities are of any practical use. LSMS calculations on copper-zinc alloys with short-range order have been published,[5] and it would be interesting to see the degree to which these could be reproduced with a PCPA that contains such order. There has been a lot of interest in the inclusion of displacements in alloy theories recently, and this is a proposal for including them in a CPA level theory.

III. COMPUTATIONAL METHODS

The computer codes used for the PCPA calculations described in this paper are based on the ones that were developed for the implementation of the LSMS method.[5,15] The supercell is first generated for the underlying face centered cubic (fcc) or body centered cubic (bcc) Bravais lattice. For bcc alloys, the dimensions of the supercell are normally chosen to be $5\times5\times5$ lattice spacings, and it contains 250 atoms. For fcc alloys, the supercell dimensions are typically $4\times4\times4$, and contain 256 atoms. The next step is to assign atoms to the lattice sites using a random number generator, with the constraint that the alloy model must have the chosen concentration. The computer code can build in short-range order as measured by the Warren-Cowley coefficients, but that capability was not used in the present work.

Ignoring static displacements of the atoms from the sites of the Bravais lattice is an approximation, but there is no reason to expect it to be a serious one for the present case. From the sharpness of the Bragg peaks and the smallness of the static Debye-Waller factors observed in diffraction experiments on metallic alloys, it is clear that, to a first approximation, the atoms fall on the sites of the average lattice. This conclusion is corroborated by the most recent experimental studies.[34] Thermal displacements are also important. At room temperature, the rms average of the thermal displacements is 3–4 times larger than the rms average of the static displacements,[35] even for alloys with a large size mismatch.

Initial guesses are made for the atomic potentials, and the t matrices are calculated. The PCPA equations in Eq. (23) are solved iteratively, using a generalization of the programs that were originally developed for use in KKR-CPA calculations. The new charge densities for each site are found using Eq. (18), and the whole process is repeated until the total energy and potentials have converged. It has been demonstrated computationally[36] that the muffin-tin approximation introduces no significant error in calculations like the ones discussed here. Even for the most extreme case, the copper-palladium alloy system, the heats of mixing calculated with muffin-tin and non-muffin-tin methods are not significantly different. That is, calculations on copper-palladium in the $L1_2$ structure with the muffin-tin LSMS method give -6.6 mRy, while the non-muffin-tin Vienna *ab initio* simulation package[37] (VASP) gives -6.8 mRy. It has been reported in the literature[38] that the non-muffin-tin linear augmented plane-wave method gives -6.3 mRy. The advantage in using the muffin-tin approximation, as compared with an atomic-sphere approximation, is that the multiple-scattering equations are exact. Questions of convergence that must be addressed when full-potential methods are used are avoided in the present approach, although such methods will be incorporated in later calculations when they are deemed necessary. As emphasized earlier, the Madelung contribution is calculated without approximation.

It might be thought that the solution of the equation for the effective scattering matrix $\mathbf{t}_c$ for the N-atom PCPA case, Eq. (23), would be much more difficult than for the isomorphous CPA, Eq. (22). It turns out that, using the standard method described in Ref. 28, only twice as many iterations were needed to solve the equation for the PCPA than for the KKR-CPA. This is due to the fact that, although the charge is different on every atom, the scattering matrices for the atoms of a given species are quite similar. The Brillouin zone integrations required when calculating τ_c^{00} were performed using the prism method[39] with 36 directions in the irreducible wedge of the Brillouin zone, which insures milli-Rydberg accuracy. All the calculations reported here were performed with the Cray T3E-900 512-processor supercomputer operated by the National Energy Research Scientific Computing Center located at the Lawrence Berkeley National Laboratory. It is, of course, always desirable to use the most powerful computing facilities that are available. However, one of

TABLE I. Convergence test of the total energy, Fermi energy, and charge transfer for a 50% copper-zinc alloy.

Supercell size	16	54	128	250
Total energy (Rv)	−3 414.465 156	−3 414.465 272	−3 414.465 129	−3 414.465 064
Fermi energy (Rv)	0.660 9	0.660 9	0.660 9	0.660 9
Charge transfer (e)	0.103 26	0.105 36	0.102 64	0.101 43

the major thrusts of our future program development is to simplify the PCPA calculations so that they can be carried out on small workstations or microcomputers.

Tests were made on the dependence of the PCPA results on N, the number of atoms in the supercell. It was found that surprisingly small samples give quite acceptable predictions for such self-averaging quantities as the total energy per atom and the charge transfer. This is illustrated by the calculations on a bcc 50% CuZn alloy with a lattice constant of 5.5 Bohr radii that are shown in Table I. The total energies calculated with supercells containing 16 and 250 atoms differ by only 92 micro-Rydbergs, and the charge transfer changes by 0.0018 electron charges. All of these supercells used in these calculations were generated randomly. This is, at the same time, a test of the sensitivity of the energy to the arrangement of the atoms in the supercell, since these samples have nothing in common except for their concentration. The Warren-Cowley short-range order parameters, other than the first, are small for these samples, which indicates that they are random. The distributions of Warren-Cowley parameters for some larger supercells are shown in Fig. 15 of Ref. 17. It is expected that unwanted order is more likely to appear in a randomly generated supercell when N is small. Such small supercells will rarely be used because PCPA calculations on large supercells are not significantly more time consuming, since the calculation of Madelung potentials with the Ewald method takes very little time.

IV. ANALYSIS OF CALCULATIONS

In Table II, experimental chemical shifts in copper-palladium, copper-zinc, and silver-palladium alloys are compared with the results of calculations using the LSMS, PCPA, and KKR-CPA. The LSMS calculations appeared in a previous publication.[29] The charge transfers predicted by the three theories are also shown. In the following, the reasons for focusing on chemical shifts rather than the densities of states that can be measured with ultraviolet photoemission spectroscopy, as was conventional in earlier evaluations of alloy theories, will be made clear.

The chemical shifts are defined as follows. In the DFT-LDA, the binding energy of a core level $E^{A,i}_{n,l}(c)$ of an A atom on site i in an A-B alloy with a concentration c is the negative of the one-electron core-level energy measured relative to the Fermi energy. The binding energy for the A atoms $E^{A}_{n,l}(c)$ is the average of the $E^{A,i}_{n,l}(c)$ over all the A sites. The binding energy for the B atoms $E^{B}_{n,l}(c)$ is defined similarly. The chemical shifts for atoms in an alloy, $\delta E^{A}_{n,l}(c)$ or $\delta E^{B}_{n,l}(c)$, are the change in the binding energy relative to the pure A or B metal. It is well understood that there are significant differences between the Koopman approximation to the binding energy and the measured binding energy of a core electron, due to the relaxation of the electrons around the core hole.[40] It has been proposed that the many-body relaxation corrections are approximately independent of concentration,[41] so they are not expected to be very important in measurements of chemical shifts.

The LSMS and PCPA calculations for the CuPd alloys shown in Table II use supercells containing 256 atoms based on fcc Bravais lattices, the lattice constant for the 50% alloy being 6.9 atomic units (au) and for the 80% alloy being 7.1 a.u. The disordered 50% CuZn alloy is in the β phase (bcc) with a lattice constant of 5.5 a.u. The supercell used with the LSMS calculations contains 432 atoms, while the one for the PCPA calculations contains 256. The ordered β' phase of

TABLE II. Experimental and theoretical values for the chemical shifts in various alloy systems. Net atomic charges calculated with the indicated theories.

Alloy	a alloy Bohr radii	atom level	Exp shift (eV)	LSMS shift (eV)	PCPA shift (eV)	KKR-CPA shift (eV)	LSMS charge ($\|e\|$)	PCPA charge ($\|e\|$)	KKR-CPA charge ($\|e\|$)
50% CuPd	7.1000	2p Cu	−0.700 00	−0.716 88	−0.856 03	−0.931 02	−0.176 09	−0.160 84	−0.043 34
		3d Pd	0.260 00	0.337 97	0.232 02	−0.006 29	0.176 09	0.160 84	0.043 84
80% CuPd	6.9000	2p Cu	−0.250 00	−0.268 17	−0.295 92	−0.323 44	−0.077 21	−0.074 53	−0.021 62
		3d Pd	0.700 00	0.654 57	0.606 68	0.436 36	0.310 87	0.299 59	0.086 48
50% CuZn	5.5000	2p Cu		0.339 58	0.225 99	0.189 42	−0.100 86	−0.101 43	−0.075 78
		2p Zn		−0.008 71	−0.133 88	0.046 90	0.100 86	0.101 43	0.075 78
CuZn $B2$	5.5000	2p Cu	0.350 00	0.568 69			−0.125 89		
		2p Zn	−0.200 00	−0.285 57			0.125 89		
50% AgPd	7.6100	3d Ag	−0.500 00	−0.477 15	−0.573 89	−0.535 90	0.049 56	0.048 63	0.057 24
		3d Pd	0.000 00	−0.101 63	−0.193 47	−0.376 86	−0.049 56	−0.048 63	−0.057 24

CuZn is in the $B2$ (CsCl) structure with the same lattice constant as the β phase. The 50% AgPd alloy is modeled with a supercell containing 256 atoms and a fcc Bravais lattice with a lattice constant of 7.61 a.u. in both the LSMS and PCPA calculations. The same lattice constants are used in the KKR-CPA calculations on all these alloy systems, but, of course, supercells are not used in such calculations. The pure metals Cu, Pd, Ag, and Zn are all taken to be fcc with lattice constants 6.7677, 7.43, 7.2744, and 7.79 a.u. The experimental chemical shifts for CuPd are taken from Ref. 42, those for CuZn are from Ref. 43, and those for AgPd are from Ref. 44. The choice of core levels listed in Table II is dictated by the existence of well-defined peaks in the energy range that can be sampled using Al $K\alpha$ or Mg $K\alpha$ x rays.

The first observation that can be made from Table II is that the chemical shifts calculated with the LSMS agree with the experimental data to within the accuracy of the experiments, as pointed out in Ref. 29. It can be concluded from this agreement that the prediction of chemical shifts in alloys is trivial in the sense that an accurate DFT-LDA calculation will yield them. Overall, the chemical shifts predicted by the PCPA calculations are very good, particularly when it is taken into account that the computational effort expended in obtaining them is a very small fraction of that required for the LSMS numbers. The effort required to calculate chemical shifts with the KKR-CPA is even less, but the agreement with experiment is further reduced.

The agreement between the LSMS calculations and experiment for such a sensitive property as the chemical shift increases the confidence that can be placed in that theory. For this reason, it is disturbing that the KKR-CPA predictions for the average charges on the constituent atoms, shown in Table II, differ considerably from the predictions of the LSMS. This is particularly noticeable for the CuPd alloys. If one takes the conventional view that chemical shifts are a measure of charge transfer, it is surprising that the chemical shifts given by the KKR-CPA are as accurate as they are. The PCPA gives values for the average charges that agree with the LSMS to within a few percent. This is expected, because the PCPA includes Coulomb effects as well as they can be within the level of a single-site approximation.

In Fig. 1, calculations of the density of states for the 50% CuPd alloy are shown. The LSMS curve is obtained by averaging the densities of states calculated for the 256 sites in the supercell. The average density of states given by the KKR-CPA is clearly different from the LSMS prediction, but it would be difficult to see differences of this magnitude in experiments. One might have expected that the difference would have been greater, given the fact that the KKR-CPA prediction of the charge transfer is only one fourth of the LSMS value. There are 10 electrons in the d bands, and the charge transfer is only 2% of that. Thus, the difference between the positions of the Fermi energies does not appear to be very large on the scale of the drawing. This explains the early successes that the KKR-CPA had in predicting the results of photoemission spectroscopy experiments, and also the reason that charge transfer and chemical shifts provide a more sensitive test of the ability of an alloy theory to treat Coulomb effects correctly.

An interesting observation that was made on the basis of data from LSMS calculations[16] is that the DFT-LDA predicts

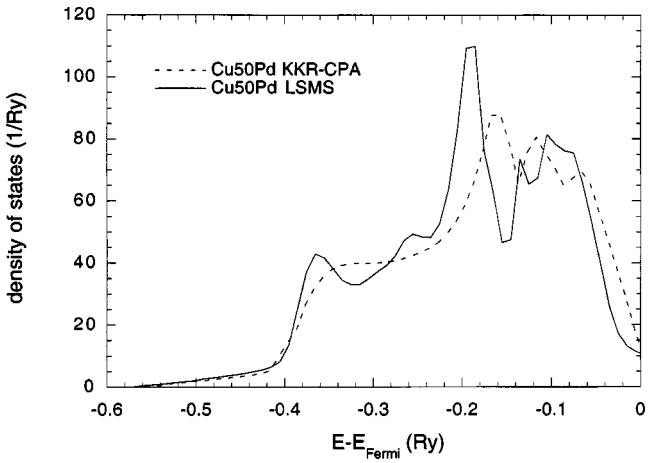

FIG. 1. The density of states of a 50% copper-palladium alloy as a function of the energy relative to the Fermi energy. The lattice constant of the fcc Bravais lattice is 6.9 atomic units. The solid line shows the average of the 256 densities of states calculated with the LSMS. The dotted line shows the density of states calculated with the standard KKR-CPA.

a linear relation between the Madelung potentials at the sites of an alloy V^i and the net charges on the sites q^i. This qV relation is not trivial because it is only true for the charges calculated in the final stage of a self-consistent calculation, while such simple conditions as charge neutrality hold at every iteration. It can be seen from Fig. 2 that the V^i and q^i from a PCPA calculation on the 50% CuPd alloy fall on lines that are as straight as the ones determined by the LSMS data. The slopes are not identical. For copper sites, the slope from the PCPA data is -1.3738 Ry/$|e|$, compared with -1.1955 from the LSMS data. For the Pd sites, the slopes are -1.2767 and -1.1826. Thus, the PCPA not only gives an accurate value for the average net charge on the atomic sites, as can be seen from Table II, but also it gives a very good description of the distribution of the charges on the sites.

Since the computer codes used for the present calculations are based on the LSMS codes, it is not difficult to extend

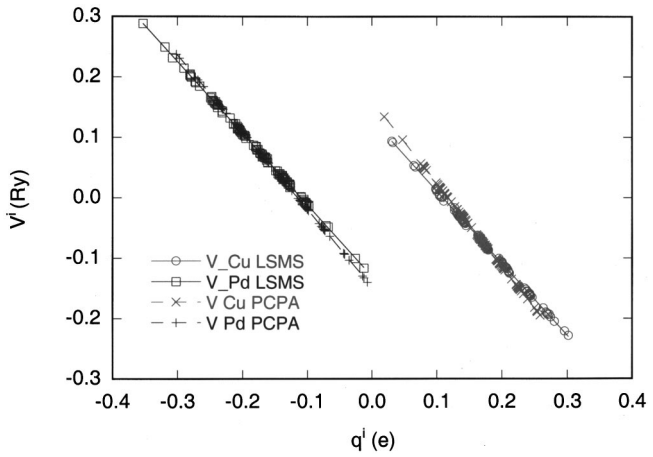

FIG. 2. The Coulomb potential at the lattice sites as a function of the net charge on the lattice sites for a 50% copper-palladium alloy. The lattice constant of the fcc Bravais lattice is 6.9 atomic units. The straight lines are the result of fits to the data. The sign convention for the charges is opposite to the one used in Table II.

them to treat LIZ's larger than one. Such LSGF calculations on the 50% CuPd alloy have been carried out with a LIZ containing 19 atoms or two nearest-neighbor shells. These calculations differ from the ones in Ref. 19 in that the multiple-scattering method is used. The improvement of the LSGF charges over the PCPA charges is not as great as might have been expected. The average net charge on the Cu atoms predicted by the calculations using $N_{\mathrm{LIZ}}=19$ is $-0.161\,53\ |e|$, only 0.4% larger than the one from the PCPA calculations. The qV relations for this alloy obtained from the LSMS and PCPA are shown in Fig. 2. The calculation using $N_{\mathrm{LIZ}}=19$ gives straight lines like the ones in the figure. The slope of the line for Cu is -1.3161 Ry/$|e|$, and for Pd it is -1.2420 Ry/$|e|$. These values are 3–4 % smaller than the ones predicted by the PCPA, and are about a third of the correction that is needed to obtain values that agree with the LSMS slopes.

V. DISCUSSION

It can be concluded that a CPA level theory that treats Coulomb effects without significant approximation exists. There are several advantages in the PCPA approach. The first is that it predicts a continuous distribution of charges about the mean for the A and B atoms, and this is in accordance with reality. The second is that there are no adjustable parameters in the theory, and this is an improvement over the isomorphous alloy theories that attempt to include nonzero Madelung potentials. The third advantage is that the inclusion of the exact form for the Madelung potentials is conceptually simpler than the approximations that have been proposed, and requires only slightly more computational effort. We emphasize that the changes to the predictions of the electronic structure obtained from other self-consistent CPA theories are quantitative but not qualitative. Those methods have had great success in explaining many properties of alloys. In hindsight, it is clear that the derivation of the Madelung potential in the KKR-CPA (Ref. 10) is logically and mathematically sound. The reason it led to a null result was the belief, generally held at that time, that the isomorphous alloy model is a necessary precondition for such derivations.

Site averaging with only the CPA conditions leads to the polymorphous PCPA. The addition of the condition that the potentials and wave functions correspond to the isomorphous model leads to the isomorphous KKR-CPA, in which the Madelung potential is zero. The isomorphous S-CPA and SIM-CPA do not fall within the algebraic sequence, although they are useful approximations. Of course, the order-N LSMS and LSGF theories give more accurate descriptions of the electronic states than any CPA, but many theoretical studies do not require so much detail.

The polymorphous nature of the PCPA leads to some interesting consequences, not all of which are explored in this paper. Not only does the PCPA give a more accurate description of the average charge transfer, it also includes fluctuations about the average. These charge fluctuations modify the density of states and the Bloch spectral density function. In particular the effects on the Bloch spectral function have the potential to change the width of peaks and, therefore, to alter electron lifetimes. This will affect calculations of such properties as the residual resistivity[45] and ordering temperatures for Fermi surface driven long period ordered structures.[46] A major problem with the isomorphous KKR-CPA is that there is no clear pathway to make the theory full potential because of difficulties with continuity of the charge density at the cell boundaries, even if one allows nonspherical corrections to the scattering. In the PCPA the fact that the Coulomb effects are treated using a supercell means that charge density is well defined throughout all space. Unfortunately, it will not be precisely continuous at the cell boundary since the multiple scattering equations are still solved in a single site approximation. How severe a restriction this imposes remains to be investigated numerically.

The development of the PCPA is only beginning, and there are many extensions that need to be carried out. A comparison of the binding energies of alloys calculated with the LSMS and KKR-CPA is given in Ref. 18. The PCPA binding energies should be added to this comparison. The formulas for $G(E,\mathbf{k},\mathbf{k})$ and hence the Bloch spectral density function $A^B(E,\mathbf{k})$ derived in Sec. II E should be utilized for calculations on some real alloys as soon as possible. The LSGF with LIZ's containing more than one atom also leads to an effective scattering matrix, $\mathbf{t}_c$. We do not consider that to be a PCPA because it is more difficult to fit it into the single-site picture, and it presupposes that one is prepared to do more time-consuming calculations. It would be interesting to compare the average Green's functions obtained using the LSGF and PCPA effective scattering matrices. The existing programs, which are based on the LSMS codes, should be simplified so that PCPA calculations can be carried out with readily available microcomputers and workstations.

ACKNOWLEDGMENTS

Work supported by Office of Basic Energy Sciences, Division of Materials Sciences and Engineering, and Office of Computational and Technology Research, Mathematical Information and Computational Sciences Division, U. S. Department of Energy, under Subcontract No. DEAC05-960R22464 with Lockheed-Martin Energy Research Corporation and DEAC03-76SF00098. B.U. and N.Y.M. were supported by an appointment to the Oak Ridge National Laboratory Postdoctoral Research Associates Program administered jointly by the Oak Ridge National Laboratory and the Oak Ridge Institute for Science and Education.

[1] Hohenberg and W. Kohn, Phys. Rev. **136**, B864 (1964); W. Kohn and L. J. Sham, Phys. Rev. **140**, A1133 (1965).
[2] L. Kaufman and H. Bernstein, *Computer Calculation of Phase Diagrams* (Academic, New York, 1970); M. Hillert and M. Schalin, J. Phase Equilib. **19**, 206 (1998).
[3] J. W. D. Conolly and A. R. Williams, Phys. Rev. B **27**, 5169 (1983); J. M. Sanchez, F. Ducastelle, and D. Gratias, Physica (Amsterdam) **128A**, 334 (1984); A. Zunger, in *Statics and Dynamics of Alloy Phase Transitions*, edited by P. E. A. Turchi and A. Gonis, Vol. 319 of *NATO Advanced Study Institute, Series B: Physics* (Kluwer, Dordrecht, 1993).
[4] R. Car and M. Parinello, Phys. Rev. Lett. **55**, 2471 (1985); M. C. Payne, M. P. Teter, D. C. Allan, T. A. Arias, and J. D. Joannopoulos, Rev. Mod. Phys. **64**, 1045 (1992); V. Godlevsky, J. R. Chelikowsky, and N. Trouillier, Phys. Rev. B **52**, 13 281 (1995); J. R. Chelikowsky, X. Jing, K. Wu, and Y. Saad, *ibid.* **53**, 12 071 (1996).
[5] Yang Wang, G. M. Stocks, W. A. Shelton, D. M. C. Nicholson, Z. Szotek, and W. M. Temmerman, Phys. Rev. Lett. **75**, 2867 (1995).
[6] J. S. Faulkner, in *Progress in Materials Science*, edited by J. W. Christian, P. Haasen, and T. B. Massalski (Pergamon, Oxford, England, 1982), Vol. 27.
[7] P. Soven, Phys. Rev. **156**, 809 (1967).
[8] J. Korringa, Physica (Amsterdam) **13**, 392 (1947); W. Kohn and N. Rostoker, Phys. Rev. **94**, 111 (1954).
[9] G. M. Stocks, W. M. Temmerman, and B. L. Gyorffy, Phys. Rev. Lett. **41**, 339 (1978).
[10] H. Winter and G. M. Stocks, Phys. Rev. B **27**, 882 (1983); D. D. Johnson, D. M. Nicholson, F. J. Pinski, B. L. Gyorffy, and G. M. Stocks, Phys. Rev. Lett. **56**, 2088 (1986); Phys. Rev. B **41**, 9701 (1990).
[11] R. Magri, S. H. Wei, and A. Zunger, Phys. Rev. B **42**, 11 388 (1990).
[12] I. A. Abrikosov, Yu. H. Vekilov, A. V. Ruban, Phys. Lett. A **154**, 407 (1991); I. A. Abrikosov, Yu. H. Vekilov, P. A. Korzhavyi, A. V. Ruban, and L. E. Shilkrot, Solid State Commun. **83**, 867 (1992).
[13] D. D. Johnson and F. J. Pinski, Phys. Rev. B **48**, 11 553 (1993).
[14] N. Papanikolao, R. Zeller, P. H. Dederichs, and N. Stefanou, Phys. Rev. B **55**, 4157 (1997).
[15] G. M. Stocks, D. M. C. Nicholson, Y. Wang, W. A. Shelton, Z. Szotek, and W. M. Temmermann, in *High Performance Computing Symposium; Grand Challenges in Computer Simulation, Proceedings of the 1994 Simulation Multiconference*, edited by A. M. Tentner (The Society for Computer Simulation, San Diego, 1994); D. M. C. Nicholson, G. M. Stocks, Y. Wang, W. A. Shelton, Z. Szotek, and W. M. Temmermann, Phys. Rev. B **50**, 14 686 (1994).
[16] J. S. Faulkner, Yang Wang, and G. M. Stocks, Phys. Rev. B **52**, 17 106 (1995); J. S. Faulkner, Yang Wang, and G. M. Stocks, in *Stability of Materials*, Vol. 355 of *NATO Advanced Study Institute, Series B: Physics*, edited by A. Gonis, P. E. A. Turchi, and J. Kudrnovsky (Plenum, New York, 1996); J. S. Faulkner, Yang Wang, Nassrin Moghadam, and G. M. Stocks, in *Properties of Complex Inorganic Solids*, edited by A. Gonis, A. Meike, and P. E. A. Turchi (Plenum, New York, 1997); J. S. Faulkner, Yang Wang, and G. M. Stocks, J. Phase Equilib. **18**, 499 (1997).
[17] J. S. Faulkner, Yang Wang, and G. M. Stocks, Phys. Rev. B **55**, 7492 (1997).
[18] J. S. Faulkner, Nassrin Moghadam, Yang Wang, and G. M. Stocks, Phys. Rev. B **57**, 7653 (1998).
[19] I. A. Abrikosov and B. Johansson, Phys. Rev. B **57**, 14 164 (1998).
[20] P. A. Korzhavyi, A. V. Ruban, I. A. Abrikosov, and H. L. Skriver, Phys. Rev. B **51**, 5773 (1995).
[21] W. Kohn, Phys. Rev. Lett. **76**, 3168 (1996).
[22] P. P. Ewald, Ann. Phys. (Leipzig) **64**, 253 (1921).
[23] I. A. Abrikosov, A. M. N. Niklasson, S. I. Simak, B. Johansson, A. V. Ruban, and H. L. Skriver, Phys. Rev. Lett. **76**, 4203 (1996).
[24] I. A. Abrikosov, S. I. Simak, B. Johansson, A. V. Ruban, and H. L. Skriver, Phys. Rev. B **56**, 9319 (1997).
[25] D. M. C. Nicholson, G. M. Stocks, W. A. Shelton, Y. Wang, and J. C. Swihart, Metall. Mater. Trans. A **29**, 1845 (1998).
[26] A. B. Oparin, D. M. C. Nicholson, X.-G. Zhang, W. H. Butler, W. A. Shelton, G. M. Stocks, and Yang Wang, J. Appl. Phys. **85**, 4548 (1999); W. H. Butler, X.-G. Zhang, T. C. Schulthess, D. M. C. Nicholson, A. B. Oparin, J. M. MacLaren, *ibid.* **85**, 5834 (1999).
[27] G. M. Stocks, B. Ujfalussy, X. Wang, D. M. C. Nicholson, W. A. Shelton, Y. Wang, and B. L. Gyorffy, Philos. Mag. B **78**, 665 (1998).
[28] J. S. Faulkner and G. M. Stocks, Phys. Rev. B **21**, 3222 (1980).
[29] J. S. Faulkner, Yang Wang, and G. M. Stocks, Phys. Rev. Lett. **81**, 1905 (1998).
[30] I. M. Lifschitz, Adv. Phys. **13**, 483 (1964).
[31] The following equations were first put forward in J. S. Faulkner, B. Ujfalussy, Nassrin Y. Moghadam, G. M. Stocks, and Yang Wang, Bull. Am. Phys. Soc. **44**, 1035 (1999).
[32] B. L. Gyorffy, Phys. Rev. B **5**, 2382 (1972).
[33] P. Lloyd, Proc. Phys. Soc. London **90**, 207 (1967).
[34] X. Jiang, G. E. Ice, C. J. Sparks, L. Robertson, and P. Zschack, Phys. Rev. B **54**, 3211 (1996); J. S. Faulkner, *ibid.* **56**, 2299 (1997).
[35] F. H. Herbstein, B. S. Borie, Jr., and B. L. Averbach, Acta Crystallogr. **9**, 466 (1956).
[36] S. G. Louie, K. Ho, and M. L. Cohen, Phys. Rev. B **19**, 1774 (1979); J. Neve, B. Sundqvist, and O. Rapp, *ibid.* **28**, 629 (1983); A. R. Jani, N. E. Brenner, and J. Callaway, *ibid.* **38**, 9425 (1988); D. M. Nicholson and J. S. Faulkner, *ibid.* **39**, 8187 (1989).
[37] G. Kresse and J. Hafner, Phys. Rev. B **47**, R558 (1993); G. Kresse and J. Furthmueller, *ibid.* **54**, 11 169 (1996).
[38] Z. W. Lu, D. B. Laks, S.-H. Wei, and A. Zunger, Phys. Rev. B **50**, 6642 (1994).
[39] G. M. Stocks, W. M. Temmerman, and B. L. Gyorffy, in *Electrons in Disordered Metals and at Metallic Surfaces*, Vol. 42 of *NATO Advanced Study Institute, Series B: Physics*, edited by P. Phariseau, B. L. Gyorffy and L. Scheire (Kluwer, Dordrecht, 1979), p. 193.
[40] A. R. Williams and N. D. Lang, Phys. Rev. Lett. **40**, 954 (1978); Phys. Rev. B **16**, 2408 (1978).
[41] M. Weinert and R. E. Watson, Phys. Rev. B **51**, 17 168 (1995).
[42] R. J. Cole, N. J. Brooks, and P. Weightman, Phys. Rev. B **56**, 12 178 (1997).
[43] G. K. Wertheim, M. Campagna, and S. Hufner, J. Phys.: Condens. Matter **18**, 133 (1974).
[44] P. Steiner and S. Hufner, Acta Metall. **29**, 1885 (1981).

[45] G. M. Stocks, and W. H. Butler, Phys. Rev. Lett. **48**, 55 (1982); W. H. Butler, and G. M. Stocks, Phys. Rev. B **29**, 4217 (1984).
[46] B. L. Gyorffy and G. M. Stocks, Phys. Rev. Lett. **50**, 374 (1983); J. Wadsworth, B. L. Gyorffy, and G. M. Stocks, in *High Temperature Alloys: Theory and Design*, edited by J. O. Stiegler (Metallurgical Society AIME, Warrendale, PA, 1984); J. B. Staunton, D. D. Johnson, and F. J. Pinski, Phys. Rev. B **50**, 1450 (1994).